One- and two-dimensional spectral diffusion of type-II excitons in InP/InAs/InP core-multishell nanowires

doi: 10.1103/PhysRevB.82.075313

One- and two-dimensional spectral diffusion of type-II excitons in InP/InAs/InP core-multishell nanowires

Yasuaki Masumoto,[1,*] Ken Goto,[1] Seitaro Yoshida,[1] Yoshiki Sakuma,[2] Premila Mohan,[3] Junichi Motohisa,[3] and Takashi Fukui[3]

[1]*Institute of Physics, University of Tsukuba, Tsukuba 305-8571, Japan*

[2]*Quantum Dot Research Center, National Institute for Materials Science, Tsukuba 305-0047, Japan*

[3]*Research Center for Integrated Quantum Electronics, Hokkaido University, Sapporo 060-8628, Japan*

(Received 2 April 2010; revised manuscript received 25 June 2010; published 12 August 2010)

Spectral diffusion of type-II excitons in InP/InAs/InP core-multishell nanowires (CMNs) and type-I excitons in an InAs/InP single quantum well (SQW) was studied by means of time-resolved and spectrally resolved photoluminescence. InP/InAs/InP CMNs in hexagonal symmetry are made of six facets and six edges which work as two-dimensional quantum wells and one-dimensional quantum wires, respectively. At 5 K type-II excitons lose their energy in two stages. In the first stage, two-dimensional spectral diffusion takes place in the type-II quantum well region in CMNs similar to spectral diffusion of type-I excitons in the InAs/InP SQW. In the second stage, slower one-dimensional spectral diffusion takes place in the quantum wire region in CMNs. Acoustic-phonon-mediated migration of excitons to lower-energy-localized states leads to the spectral diffusion in two dimensions and one dimension.

DOI: 10.1103/PhysRevB.82.075313 PACS number(s): 78.67.Ch, 71.35.−y, 78.47.da

Carrier localization in the disordered system depends highly on dimensionality and size. A sharp mobility edge is present for transport in three dimensions while is absent in two dimensions.[1] Optical spectroscopy has revealed inhomogeneous broadening of excitons, exciton localization, exciton mobility edge, and exciton spectral diffusion in the disordered system. In fact, spectral diffusion of excitons is widely observed in inhomogeneously broadened exciton bands of quasi-two-dimensional quantum wells (QWs) (Refs. 2–4) and three-dimensional mixed crystals.[5,6] Exciton localization, delocalization, and mobility edge are reported in quasi-two-dimensional QW.[7] Usually observed features are (1) photoluminescence (PL) decay becomes gradually slower with decrease in the photon energy and (2) time-resolved PL spectrum is gradually shifted toward lower energy as time proceeds. Spectral diffusion is believed to take place by the acoustic-phonon-mediated spatial transfer of excitons localized in the fluctuated potential.

It is expected that spectral diffusion highly depends on the dimensionality. In three dimensions, spatial transfer of excitons localized in the fluctuated potential is not difficult, because localized excitons can find the nearby sites with very small energy mismatch. On the other hand, in one dimension, it is difficult because of the limited path for the spatial transfer. Dimensionality-dependent spectral diffusion is predicted theoretically[8] but has not been studied experimentally. Quantum structures having both two-dimensional QWs and one-dimensional quantum wires (QWRs) are idealistic system for the study of the dimensionality-dependent spectral diffusion. In this work, we study type-II exciton dynamics in wurtzite InP/InAs/InP core-multishell nanowires (CMNs) composed of two-dimensional QWs and one-dimensional QWRs and type-I exciton dynamics in an InAs/InP single QW (SQW) by using time-resolved and spectrally resolved PL. It is also needed to understand the similarity or difference in the spectral diffusion of type-I excitons and type-II excitons. The scope of the study is to observe two-dimensional and one-dimensional spectral diffusion and the similarity or the difference in spectral diffusion of type-I excitons and type-II excitons.

We studied two kinds of InAs/InP nanostructurs. One kind of them, InP/InAs/InP CMNs, have unique nanostructures in hexagonal symmetry.[9,10] As is schematically shown in Fig. 1(a), an ultrathin wurtzite InAs hexagonal tube a few monolayer (ML) thick is surrounded by an inner thick wurtzite InP hexagonal pillar (core) and an outer thick wurtzite InP hexagonal tube (shell). Lattice constants of free-standing wurtzite InAs and InP are a(InAs)=0.42 nm, c(InAs)=0.69 nm and a(InP)=0.40 nm, c(InP)=0.66 nm, respectively. Thickness of the InAs hexagonal tube, a few MLs, is less than the critical thickness for the onset of strain relaxation[11] and therefore the ultrathin InAs hexagonal tube is considered to be coherently strained in all directions and to be in nearly hydrostatic strain field. Model-solid theory by Van de Walle[12] explains that nearly hydrostatic strain field forms type-II band lineup.[13] Hole wave function confined in the InAs layer and its quantized energy are calculated by solving effective-mass Schrödinger equation on the finite element method with triangular array of 24 888 nodes for 1/6 section of the InAs hexagonal tube surrounded by inner and outer InP layers. The squared amplitude of the calculated hole envelope functions is displayed in Fig. 1(a). The lowest energy state is the bonding sum of wave functions peaked at the corners which is almost degenerate with the antibonding sum of them. The next lowest energy state is the bonding sum of wave functions peaked at the sides which is higher than the lowest energy state by 3 meV. Lateral extent of absolute squared wave function at the corner has the half width at half maximum of 4 nm which is ~11% of the side length 35 nm long and that at the side has the half width at half maximum of 12.5 nm which is ~36% of the side length. This shows the quantized energy at the corner is lower than that at the side by 3 meV, and two-dimensional type-II QWs and one-dimensional type-II QWR are formed in the ultrathin InAs

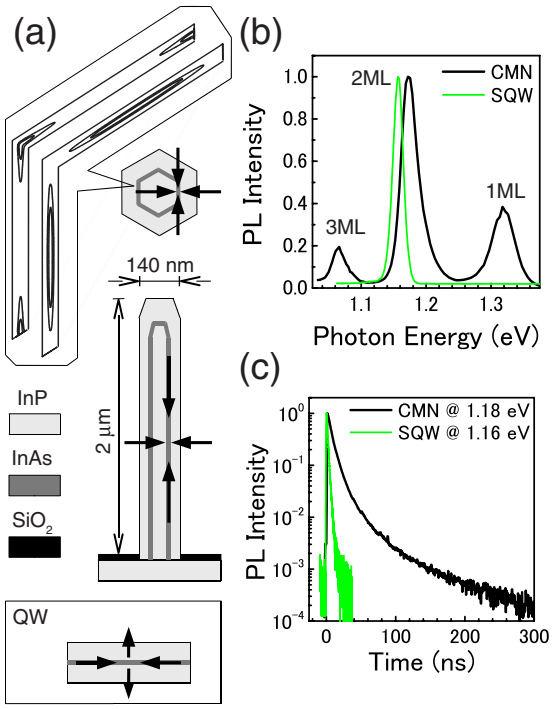

FIG. 1. (Color online) (a) Structure and strain in an InP/InAs/InP CMN and an InAs/InP SQW. The absolute square of the eigenwave functions of the first and the second lowest-energy holes in a CMN are plotted in contour maps. (b) PL spectrum of CMNs and a SQW at 5 K under the excitation at 1.88 eV. PL spectrum of CMNs consists of a band of one InAs monolayer (1 ML), a band of two InAs monolayers (2 ML), and a band of three InAs monolayers (3 ML). (c) Temporal change of 2 ML PL in CMNs and a SQW at 5 K. At 820 kHz repetition rate, 2 ps pulses at the excitation photon energy of 1.18 eV and 1.16 eV selectively excite ultrathin wurtzite InAs tubes and a zincblende InAs SQW, respectively. Time-resolved PL measurement is done by means of single photon counting.

hexagonal tube.[14,15] The PL spectrum of InP/InAs/InP CMNs shown in Fig. 1(b) contains bands of type-II excitons consisting of holes in the InAs ultrathin, strained hexagonal tube and electrons in the InP core or the InP outer shell.[13] Large Stokes shift between PL and PL excitation (PLE) spectra[13] and slow decay of PL with a decay tail lasting up to 300 ns indicate a type-II band lineup, as is shown in Fig. 1(c). Spectra of PL and PLE are composed of multiple bands due to ML scale variation in the InAs layer thickness. Multiple bands in macroscopic PL and PLE are much broader than the lifetime broadening and are inhomogeneously broadened. Further single wire spectroscopy confirms that multiple bands and inhomogeneous broadening exist even in a single wire[16] and that polarization of PL is perpendicular to the wire axis consistently with the wurtzite crystal structure.[17] Inhomogeneous broadening is considered to arise in a wire due to short-range roughness at the interface. Disorder-induced potential fluctuation causes localization of type-II excitons in both QW and QWR.[16,18]

We studied another kind of InAs/InP nanostructure, a zincblende InAs/InP SQW 2 ML thick, as a reference. Although biaxial compressive strain $\epsilon_{\mathrm{InAs}\parallel}=-0.0345$ is applied

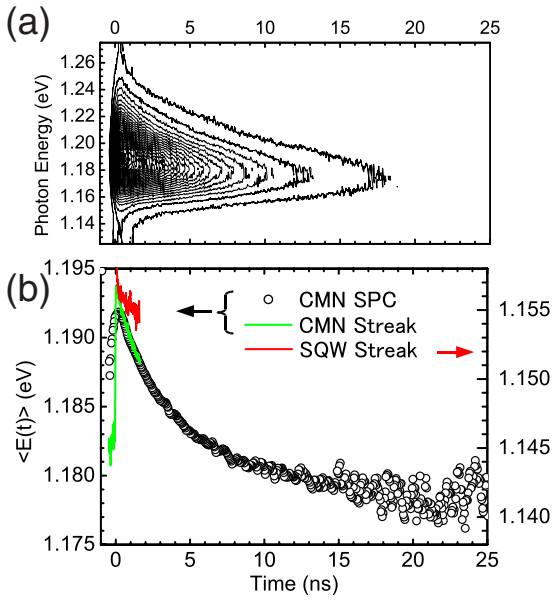

FIG. 2. (Color online) (a) Contour map of time-resolved and spectrally resolved 2 ML PL in InP/InAs/InP CMNs at 5 K. Ultrathin wurtzite InAs tubes were selectively excited by 2 ps pulses at 1.377 eV and 820 kHz. Time-resolved PL measurement is done by means of single photon counting. (b) The average energy of time-resolved and spectrally resolved 2 ML PL in CMNs shown in (a) is plotted by open circles. The average energies of time-resolved and spectrally resolved 2 ML PL in CMNs and PL in a 2 ML InAs/InP single quantum well taken by a streak camera are plotted by solid lines. All the data are the five adjacent averages of the raw data.

to a thin InAs layer along the interface, uniaxial tensile strain $\epsilon_{\mathrm{InAs}\perp}=0.0376$ is perpendicular to the interface, and the InAs layer is elongated in the direction, as is schematically shown in Fig. 1(a). According to the model-solid theory,[12] the strain gives $\Delta E_v=0.40$ eV and $\Delta E_c=0.39$ eV to the valence-band discontinuity and the conduction-band discontinuity, respectively. As a result, the SQW 2 ML thick behaves as type-I QW.[19] It shows a PL band at 1.16 eV at 5 K and fast decay of PL with a time constant of 1.7 ns, as is shown in Figs. 1(b) and 1(c).[20]

Time-resolved PL of InP/InAs/InP CMNs and an InAs/InP SQW was measured at 5 K under the excitation of mode-locked Ti:sapphire laser at 1.377 eV. Excitation photon energy of 1.377 eV excites InAs selectively. The excitation density was as low as 1.6 μJ/cm^2. Single photon counting with an InGaAsP photomultiplier was used up to 40 ns while an infrared (S1) streak camera was used up to 1.6 ns. The former has time resolution of 1 ns while the latter has better time resolution of 10 ps. The macroscopic PL spectrum shows multiple bands due to ML scale variation in the InAs layer thickness and inhomogeneous broadening of ~42 meV, as is shown in Fig. 1(b). Time-resolved and spectrally resolved 2 ML-PL band is shown in Fig. 2(a) and the time-dependent average energy of type-II excitons in Fig. 2(b). Average energy for the 2 ML band is calculated to be $\langle E(t)\rangle=[\int EI_{\mathrm{PL}}(E,t)dE]/[\int I_{\mathrm{PL}}(E,t)dE]$, where $I_{\mathrm{PL}}(E,t)$ is the PL intensity measured at energy E and time t. Integral ranges from 1.142 to 1.268 eV for the 2 ML-PL band of CMNs and from 1.136 to 1.181 eV for the 2 ML-PL band of the SQW.

The average energy of 2 ML PL of CMNs decreases initially at the rate of 4×10^6 eV/s and the energy-loss rate slows down later. Slow time-dependent redshift of PL is interpreted as slow spectral diffusion of type-II excitons due to acoustic-phonon-mediated relaxation of excitons between the localized states within the inhomogeneous broadening. Slow time-dependent redshift of PL is also observed in the 2 ML-SQW. Between 0.3 and 1.6 ns, the energy-loss rate of type-I excitons in the 2 ML-SQW is twice slower than that of type-II excitons in CMNs.

In some CMNs, islands 2 ML thick as well as islands 1 ML thick coexist, as are proved by single wire spectroscopy.[16] The exciton migration from 1 ML islands to 2 ML islands is considered to take place in them earlier. The energy difference between the 1 ML PL band and the 2 ML PL band is about 140 meV which is far beyond the acoustic phonon energy and is 4.7 times of longitudinal optical (LO) phonon energy (30 meV) in InAs and 3.1 times of LO phonon energy (45 meV) in InP. The exciton migration is considered to be associated with LO phonon emission and to be faster than the present time resolution.[21] In this work we discuss the slow exciton migration in 2 ML PL band alone.

The spectral diffusion of type-II excitons can be evaluated by exciton-phonon interaction Hamiltonian for the localized type-II exciton. However, there was no theoretical work to deal with it. In the previous paper,[22] we discussed it by referring spectral diffusion theory for the localized type-I exciton. The most essential points are that the envelope function of the type-I exciton and that of the type-II exciton are written by the same form and that only the z-axis component is different between them, where z axis is taken to be perpendicular to the heterointerface. The quasi-two-dimensional exciton-phonon interaction Hamiltonian for the deformation-potential coupling depends on the common envelope function of the type-I exciton and the type-II exciton at the small limit of the well thickness and therefore has the same expression for the type-I exciton and the type-II exciton.

In the QW and QWR regions in CMNs, an InAs layer is considered to consist of a number of clusters in which the layer width is constant and multiples of atomic layer thickness. Excitons are localized in respective clusters and the lateral size of each cluster is smaller than in-plane diameter of the exciton because the PL spectrum of excitons in a single CMN does not show substructures, as is seen in Fig. 1 of Refs. 16 and 22. Localized excitons are characterized by the Gaussian localization length ξ. Excitons are assumed to lose their energy slowly via the acoustic-phonon-mediated intercluster transfer process of long-range dipole-dipole type and short-range tunneling type. Time-dependent perturbation theory derives the major acoustic-phonon-mediated intercluster transfer rate due to the deformation-potential-type exciton-phonon interaction by the quasi-two-dimensional exciton-phonon interaction Hamiltonian. It is proportional to the following term:[23]

$$(T+J)\exp\left[-\frac{\xi^2Q^2}{2}\right]\times\left[\frac{D_c}{[1+(\alpha_hQ/2\alpha)^2]^{3/2}}-\frac{D_v}{[1+(\alpha_eQ/2\alpha)^2]^{3/2}}\right]^2, \quad (1)$$

where exciton diffusion takes place by the acoustic-phonon-mediated spatial transfer of the short-range tunneling type $T\propto\exp(-r^2/4\xi^2)$ and the transfer of the long-range dipole-dipole type $J\propto r^{-6}$ between localized states separated by a distance r, $D_c(D_v)$ is the deformation potential for the conduction (valence) band, $1/\alpha$ is the lateral extent of the exciton envelope function along the QW interface, $\alpha_{e(h)}=m_{e(h)}/(m_e+m_h)$ is given by the mass of electron m_e and the mass of hole m_h, and Q is the wave vector of phonons. The term in Eq. (1) shows that localized excitons can only interact with phonons whose wave vectors Q are smaller than the inverse of the localization extent of excitons $1/\xi$ which is estimated to be in an order of $(10\ \text{nm})^{-1}=10^6\ \text{cm}^{-1}$.[3,24] As a result, only small-energy long-wavelength phonons with $\hbar u/\xi$ (<1 meV) participate in the energy relaxation of localized excitons where u is the sound velocity. For the small-energy long-wavelength phonons, the second big bracket in Eq. (1) is reduced to $(D_c-D_v)^2$. In this limit, the intercluster transfer rate due to the deformation-potential-type exciton-phonon interaction is proportional to $(D_c-D_v)^2$ not only in two dimensions but also in three dimensions.[24] The same story holds in one dimension. We can neglect the intercluster transfer rate due to the piezoelectric-type exciton-phonon interaction in CMNs.[22]

In Fig. 2(b), we can find that the energy-loss rate becomes slower gradually. Around 10 ns, the energy-loss rate slows down. We consider that the energy-loss rate depends on the dimensionality of the region where excitons are localized. The energy-loss process of excitons is considered as follows. The excitons, confined in the QW region in the InP/InAs/InP side heterointerface in the CMN, can find the nearby and lower energy clusters in the QW region more easily than those in the QWR region and migrate toward the lower energy positions in an inhomogeneous well, when the exciton energy is not lowest. On the other hand, the excitons localized in the QWR region at the corner heterointerface in the CMN move predominantly one dimensionally. This is because the energy in the corner region is lower than that in the side region by 3 meV. In the above-mentioned scenario, the spectral diffusion took place in two stages: the first (second) energy-loss rate indicates the two-(one-) dimensional spectral diffusion. To put it another way, the photoexcited excitons localized in the CMN migrate from the side of the CMN toward the corner of the CMN.

Dimensionality-dependent spectral diffusion is discussed by considering the number of lower energy localized sites in d-dimensional sphere to which the exciton spatial transfer is possible.[8] Exciton diffusion takes place by the transfer of the short-range tunneling type and the transfer of the long-range dipole-dipole type. The latter is predominant, because of the major contribution of the long-range spatial integration.[23]

Then we consider the dipole-dipole-type exciton transfer alone and simplify the transfer rate Eq. (1) to $1/\tau(r)$ between sites separated by a distance r written by

$$1/\tau(r)=A/r^6. \quad (2)$$

It means excitons can be transferred by a distance $r(t)=(At)^{1/6}$ at the time t. The distance $r(t)$ increases with increase in time t very slowly. Excitons migrate among localized states whose density is represented by $N_dg_d(E)$,

where N_d is the density of localized states in d dimension and $g_d(E)$ is the normalized density of localized states in d dimension satisfying the normalization $\int_0^\infty g_d(E)dE=1$, where E denotes the redshift energy of excitons and is taken to be positive toward the lower photon energy side.[25] At the lowest temperature, excitons at the redshift energy ΔE can be transferred to the lower-photon-energy (larger redshift energy) sites having the density $N_d\int_{\Delta E}^\infty g_d(E)dE$ and in a d-dimensional sphere of radius $r(t)$ with the volume $V_d[r(t)]$ expressed by $\pi r(t)^2$ and $2r(t)$ for $d=2$ and 1, respectively. Therefore

$$\int_{\Delta E}^{\infty} g_d(E)dE = \frac{1}{N_d V_d[r(t)]} \tag{3}$$

holds for arbitary $g_d(E)$. It gives the relation between ΔE and t depending on dimensionality. Because PL spectrum is well approximated by a Gaussian function, $g_d(E)=g_{d0}\exp[-4\ln 2(E-E_{d0})^2/w_d^2]$, where a band full width of $w_1=w_2=42$ meV are assumed for localized states in the QW region of the InP/InAs/InP side heterointerface and the QWR region of the corner heterointerface in the CMN reflecting the bandwidth of the PL spectrum shown in Fig. 1(b). Here $E_{10}-E_{20}=3$ meV is assumed because of the energy difference between QW and QWR in CMN. The temporal change in the average energy of PL is shown as a function of time in the logarithmic scale in Figs. 3(a) and 3(b), and the energy-loss rate is slowed down around 10 ns. The experimental energy loss of excitons is fitted by a set $(\Delta E,t)$ obtained from Eq. (3) with dimensionless parameters, $\pi(At)^{1/3}N_2=3.38$ and $2(At)^{1/6}N_1=2.70$ at $t=10$ ns and $E_{10}=2$ meV. Good agreement between experimental energy loss and calculated energy loss in both two dimensions and one dimension is obtained.[26]

It means that energy-loss rate depends on the dimensionality and that the one-dimensional energy-loss rate is slower than the two-dimensional energy-loss rate. Good fitting is obtained. Intuitive picture of the crossing is that lower energy localized states can be found only in QWR at lowest energy because of the energy difference between QW and QWR in CMN. We think exciton diffusion takes place two dimensionally before 10 ns and later one dimensionally.

As was described theoretically, the spectral diffusion of two-dimensional excitons depends little on whether excitons are type I or Type II. In the type-I exciton, both the electron and the hole are confined in the well layer while in the type-II exciton, the electron and the hole are localized in different layers. The deformation potentials of the valence (conduction) band of InAs and InP are given as 1.00 eV (−5.08 eV) and 1.27 eV (−5.04 eV), respectively.[12] The difference in the deformation potentials of the valence (conduction) band between InAs and InP is very small. In the case of the type-I exciton, both the electron and the hole are confined in the InAs well layer, and the difference in the deformation potential between the conduction band and the valance band is −6.08 eV (=−5.08 eV−1.00 eV). On the contrary, in the case of the type-II exciton, where the hole is confined in the InAs well layer and the electron is localized in the InP barrier layer, the difference in the deformation potential between the conduction band and the valance band is −6.04 eV (=−5.04 eV−1.00 eV). This is different from the deformation potential for the type-I exciton by only 0.7%. Therefore, the type-I exciton-deformation potential interaction is almost the same as the type-II exciton-acoustic phonon deformation potential interaction in an InAs/InP SQW. Therefore, we can take the same A in Eq. (2) for type-I excitons in the InAs/InP SQW and type-II excitons in InP/InAs/InP CMNs. We used a Gaussian function, $g_d(E)=g'_{20}\exp[-4\ln 2(E-E_{20})^2/w_2'^2]$, where a band full width of $w_2'=19$ meV are assumed for localized states in the InAs/InP SQW from the bandwidth of the PL spectrum shown in Fig. 1(b). The experimental energy loss of type-I excitons in the SQW is well fitted by a set $(\Delta E,t)$ obtained from Eq. (3) with a dimensionless parameter $\pi(At)^{1/3}N_2=2.59$ at $t=1$ ns. As is seen in Fig. 1(b), PL spectrum of CMNs is twice broader than that of the SQW. Therefore, energy-loss rate of excitons in CMNs is twice faster than that of the SQW, as is seen in Figs. 2 and 3(b). The energy-loss rate depends on the bandwidth of the localized states, as is observed earlier.[3]

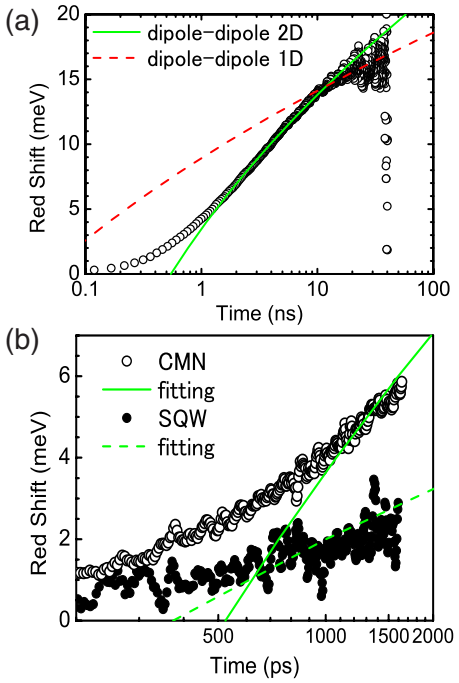

FIG. 3. (Color online) Redshift of the average energy of PL versus time in a logarithmic scale ranging (a) from 0.1 to 40 ns and (b) from 200 to 1600 ps. The average energy is given by the five adjacent averages of the raw average energies. (a) A solid line shows fitting on a model of dipole-dipole-type two-dimensional spectral diffusion and a dashed line shows fitting on a model of dipole-dipole-type one-dimensional spectral diffusion. (b) A solid line and a dashed line show fitting to redshift of the average energy of PL in the InP/InAs/InP CMN and the InAs/InP SQW, respectively, on a model of dipole-dipole-type two-dimensional spectral diffusion.

In summary, time-resolved and spectrally resolved PL measurement revealed spectral diffusion of type-II excitons in wurtzite InP/InAs/InP CMNs. The spectral diffusion takes place in two stages in the inhomogeneously broadened PL

band of a CMN. The spectral diffusion in the earlier stage took place at an initial energy-loss rate of 4×10^6 eV/s similarly to spectral diffusion of type-I excitons in the InAs/InP SQW and is ascribed to two-dimensional diffusion of type-II excitons in the InP/InAs/InP side heterointerface embedded in the CMN. The spectral diffusion in the later stage is ascribed to one-diemnsional diffusion of type-II excitons in the InP/InAs/InP corner heterointerface embedded in the CMN. This suggests that photoexcited excitons in a core-multishell nanowire move from the two-dimensional side heterointerface in the nanowire toward the one-dimensional corner heterointerface in the nanowire. Acoustic-phonon-mediated migration of exciton to lower-energy-localized states leads to the spectral diffusion in two dimensions and one dimension at low temperatures.

Authors are indebted to T. Takagahara at Kyoto Insitute of Technology for the theoretical extension of the spectral diffusion of the type-I excitons to that of the type-II exciton, and S. Watanabe at the University of Tokyo and K. Hino at University of Tsukuba for the finite element calculation of the hole wave function in the InAs layer in this work. This work was supported by Grant-in-Aid for Scientific Research No. 20244044 from the MEXT of Japan and R&D promotion scheme funding international joint research promoted by NICT of Japan.

*shoichi@sakura.cc.tsukuba.ac.jp; http://www.sakura.tsukuba.ac.jp/~masumoto/

[1] E. Abrahams, P. W. Anderson, D. C. Licciardello, and T. V. Ramakrishnan, Phys. Rev. Lett. **42**, 673 (1979).

[2] Y. Masumoto, S. Shionoya, and H. Kawaguchi, Phys. Rev. B **29**, 2324 (1984).

[3] Y. Masumoto, S. Shionoya, and H. Okamoto, Proceedings of the 17th International Conference on the Physics of Semiconductors, edited by J. D. Chadi and W. A. Harrison (Springer, New York, 1985), p. 349.

[4] J. F. Donegan, R. P. Stanley, J. P. Doran, and J. Hegarty, J. Lumin. **58**, 216 (1994).

[5] C. Gourdon and P. Lavallard, Phys. Status Solidi B **153**, 641 (1989).

[6] E. Cohen and M. D. Sturge, Phys. Rev. B **25**, 3828 (1982).

[7] J. Hegarty, L. Goldner, and M. D. Sturge, Phys. Rev. B **30**, 7346 (1984).

[8] L. E. Golub, E. L. Ivchenko, and A. A. Kiselev, J. Opt. Soc. Am. B **13**, 1199 (1996).

[9] P. Mohan, J. Motohisa, and T. Fukui, Appl. Phys. Lett. **88**, 133105 (2006).

[10] P. Mohan, J. Motohisa, and T. Fukui, Nanotechnology **16**, 2903 (2005).

[11] J. Cibert, Y. Gobil, L. S. Dang, S. Tatarenko, G. Feuillet, P. H. Jouneau, and K. Saminadayar, Appl. Phys. Lett. **56**, 292 (1990).

[12] C. G. Van de Walle, Phys. Rev. B **39**, 1871 (1989).

[13] B. Pal, K. Goto, M. Ikezawa, Y. Masumoto, P. Mohan, J. Motohisa, and T. Fukui, Appl. Phys. Lett. **93**, 073105 (2008).

[14] G. Ferrari, G. Goldoni, A. Bertoni, G. Cuoghi, and E. Molinari, Nano Lett. **9**, 1631 (2009).

[15] We can simply understand that the energy is lower at the corners than that at the sides, by considering that InAs well can be $2/\sqrt{3}$ times thicker at the corners than at the sides. Electronic states in a hexagonal tube with rounded edges were calculated by Ref. 14. The lowest energy state is the bonding sum of wave functions localized at the corners and six lowest-energy states are displayed. If wurtzite InP/InAs/InP CMNs have perfect hexagonal symmetry in the atomic level, linear combinations of wave functions shown in Fig. 1(a) with sixfold rotation are the eigenfunctions for holes. Then hole bands are formed. The linear combinations of wave functions in CMNs are shown on a simplified model in Ref. 14.

[16] K. Goto, M. Ikezawa, S. Tomimoto, B. Pal, Y. Masumoto, P. Mohan, J. Motohisa, and T. Fukui, Jpn. J. Appl. Phys., Part 1 **48**, 04C203 (2009).

[17] Y. Masumoto, K. Goto, Y. Hirata, P. Mohan, J. Motohisa, and T. Fukui (unpublished).

[18] B. Pal, K. Goto, M. Ikezawa, Y. Masumoto, P. Mohan, J. Motohisa, and T. Fukui, J. Lumin. **129**, 1941 (2009).

[19] M. Hopkinson, J. P. R. David, P. A. Claxton, and P. Kightley, Appl. Phys. Lett. **60**, 841 (1992).

[20] The same decay time constant was obtained by time-resolved up-conversion measurement, too: S. Tomimoto, A. Kurokawa, Y. Sakuma, T. Usuki, and Y. Masumoto, Phys. Rev. B **76**, 205317 (2007).

[21] We applied the up-conversion PL time-resolved spectroscopy (time resolution=120 fs) to both the 1 ML PL band and the 2 ML PL band under the excitation at 1.41 eV and found no difference in the rise of PL. This fact suggests the exciton migration from 1 ML islands to 2 ML islands takes place earlier than 120 fs.

[22] Y. Masumoto, K. Goto, B. Pal, P. Mohan, J. Motohisa, and T. Fukui, Physica E (to be published).

[23] T. Takagahara, J. Lumin. **44**, 347 (1989).

[24] T. Takagahara, Phys. Rev. B **31**, 6552 (1985).

[25] H. Kalt, J. Collet, S. D. Baranovskii, R. Saleh, P. Thomas, L. S. Dang, and J. Cibert, Phys. Rev. B **45**, 4253 (1992).

[26] Because the PL spectrum is well fitted by the Gaussian density of localized states, we use the Gaussian density of localized states and calculate Eq. (3) numerically. To give the intuitive and instructive picture to the dimensionality-dependent energy loss, we can use the exponential tail for the localized states to calculate Eq. (3) analytically. Tentatively assuming the density of the localized states as the exponential tail $g_d(E)=g_0\exp(-E/\epsilon)$ for large E, we obtain $g_0\epsilon\exp(-\Delta E/\epsilon)$ for the integral in Eq. (3). Then Eq. (3) leads to $\Delta E=\epsilon\ln(2g_0N_1\epsilon)+(\epsilon/6)\ln(At)$ for one dimension and $\Delta E=\epsilon\ln(\pi g_0N_2\epsilon)+(\epsilon/3)\ln(At)$ for two dimensions. Then $d\Delta E/d\ln(At)=\epsilon d/6$. It analytically shows the slope of two-dimensional energy loss versus $\ln(t)$ is twice of the slope of one-dimensional energy loss versus $\ln(t)$, as is seen in Fig. 3.